ADVANCED MATERIALS
www.advmat.de

Complementary Logic Circuits Based on High-Performance n-Type Organic Electrochemical Transistors

*Hengda Sun, Mikhail Vagin, Suhao Wang, Xavier Crispin, Robert Forchheimer, Magnus Berggren, and Simone Fabiano**

Organic electrochemical transistors (OECTs) have been the subject of intense research in recent years. To date, however, most of the reported OECTs rely entirely on p-type (hole transport) operation, while electron transporting (n-type) OECTs are rare. The combination of efficient and stable p-type and n-type OECTs would allow for the development of complementary circuits, dramatically advancing the sophistication of OECT-based technologies. Poor stability in air and aqueous electrolyte media, low electron mobility, and/or a lack of electrochemical reversibility, of available high-electron affinity conjugated polymers, has made the development of n-type OECTs troublesome. Here, it is shown that ladder-type polymers such as poly(benzimidazobenzophenanthroline) (BBL) can successfully work as stable and efficient n-channel material for OECTs. These devices can be easily fabricated by means of facile spray-coating techniques. BBL-based OECTs show high transconductance (up to 9.7 mS) and excellent stability in ambient and aqueous media. It is demonstrated that BBL-based n-type OECTs can be successfully integrated with p-type OECTs to form electrochemical complementary inverters. The latter show high gains and large worst-case noise margin at a supply voltage below 0.6 V.

Organic electrochemical transistors (OECTs) have attracted great attention as they hold significant promise for a variety of applications ranging from printable logic circuits for electronic textiles to drivers for sensors and flat panel display pixels, as well as to artificial synapse for neuromorphic computing.[1] Because of the low working bias, high sensitivity, and stability in aqueous environments, as well as biological and mechanical compatibility with live tissues, OECTs have also recently emerged as a technological solution to a variety of diagnostic and therapeutic applications.[2] A considerable amount of work has focused, for example, on approaches exploiting the principle of OECTs for the development of biomedical tools for chemical and biological sensing,[3] electrophysiological recording,[4] monitoring of cell viability, and barrier tissue integrity,[5] to name just a few. In an OECT, the electroactive polymer constituting the channel is in direct contact with an electrolyte and with the source and drain metal electrodes (**Figure 1**A). Because of the soft and permeable nature of the electroactive polymers, ions are able to penetrate into the bulk of the transistor channel.[6] The operation of an OECT relies then on a reversible ion exchange and charge compensation process, which leads to a bulk doping of the organic conducting channel and to a modulation of the electronic conductivity between the source and drain contacts. Hence, OECTs transduce a modulation in the gate voltage (V_G) to a modulation in the drain current (I_D) running through the entire bulk of the channel. The figure-of-merit that quantifies the efficiency of this transduction is the transconductance, defined as $g_m = \partial I_D/\partial V_G$.

The current state-of-the-art active material for OECTs is the mixed ion-electron conducting polymer poly(3,4-ethylenedioxythiophene):poly(styrenesulfonate) (PEDOT:PSS). The volumetric doping and dedoping of PEDOT:PSS result in a modulation of the drain–source current of several orders of magnitude with a consequent high transconductance.[7] As PEDOT:PSS is doped in its pristine state, and thus highly conducting, the OECT operates in depletion mode. In addition, several polythiophene-based polymers have been reported as efficient electroactive channel materials for enhancement mode OECTs.[8] To date, however, essentially all reported OECTs have relied on hole transport (p-type), while the development of electron

Dr. H. Sun, Dr. M. Vagin, Dr. S. Wang, Prof. X. Crispin, Prof. M. Berggren, Dr. S. Fabiano
Laboratory of Organic Electronics
Department of Science and Technology
Linköping University
SE-601 74 Norrköping, Sweden
E-mail: simone.fabiano@liu.se
Dr. M. Vagin
Department of Physics
Chemistry and Biology
Linköping University
SE-581 83 Linköping, Sweden
Prof. R. Forchheimer
Department of Electrical Engineering
Linköping University
SE-581 83 Linköping, Sweden

The ORCID identification number(s) for the author(s) of this article can be found under https://doi.org/10.1002/adma.201704916.

DOI: 10.1002/adma.201704916

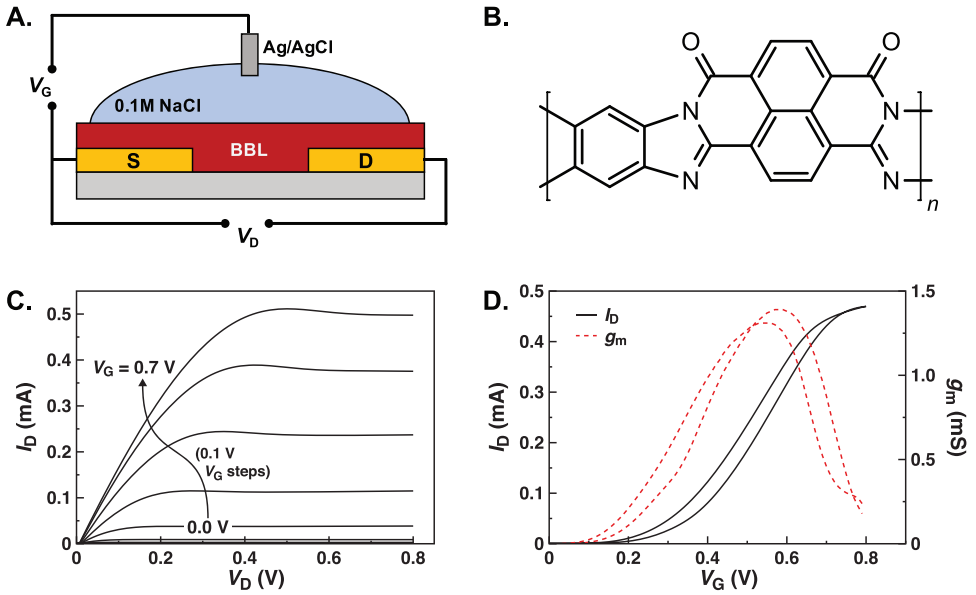

Figure 1. A) Cross-sectional schematic of the OECT. B) The chemical structure of BBL. C) Output characteristics of a BBL-based OECT (W = 39 mm, L = 20 µm, d = 20 nm) with gate voltage ranging from 0 to 0.7 V in steps of 0.1 V. D) Transfer characteristics of the same device and the corresponding transconductance (g_m) values at V_D = 0.6 V.

transporting (n-type) OECTs has been almost entirely disregarded. Efficient n-type OECTs are of paramount importance as they would allow for a dramatic sophistication of bioelectronics devices and complementary logic circuits. However, this development is hold back primarily by the lack of appropriate semiconductor materials: it necessitates a material that can be reversibly reduced and oxidized in aqueous media. This then requires the design of materials that have a high electron affinity (EA).[9] In addition to their ability to be oxidized and reduced reversibly and efficiently, these materials should also have high electron mobilities in order to support large electronic currents and yield large current modulation when included as the channel of an OECT. Recently, a first example of n-type OECT comprising a naphthalene diimide (NDI) based donor–acceptor polymer was reported, exhibiting relatively balanced hole and electron transport characteristics.[10] However, despite the high EA, NDI-based polymers typically suffer from a low water stability,[11] and proper side chain and/or backbone engineering is necessary for a stable operation in aqueous media.[10,12] In addition, when doped, NDI-based polymers suffer from a limited electron conductivity due to the highly localized nature of the charge carriers on the chains as the result of the donor–acceptor character.[13] Consequently, currents and transconductance of NDI-based OECTs are limited when compared with the traditional accumulation mode p-type counterparts. We have recently demonstrated that solution-processable ladder-type conducting polymers, such as the n-type poly(benzimidazobenzophenanthroline) (BBL)[14] (Figure 1B), can achieve electron conductivities that are three orders of magnitude higher than those measured for distorted NDI-based donor–acceptor polymers.[15] This was ascribed to the high rigidity and planarity of the π-conjugated polymer backbone, which promotes delocalization of the carriers in BBL making intramolecular transfer easier, thus providing high polaron mobility along the ladder-type chain.[15] Furthermore, BBL features integrated redox active sites, which ensure high n-dopability, typical of π-conjugated redox polymers.[16]

Here, we show that ladder-type conducting polymers such as BBL can work efficiently as the electroactive channel of electrochemical transistors. We report accumulation mode BBL-based transistors with record-high transconductance for an n-type OECT. Thanks to the high electron conductivity and EA of BBL, the OECTs here reported operate at high current levels and modulation in water medium, and show high stability during pulse measurements over 1 h of continuous operation. Moreover, we measure a remarkable ambient stability over three months of storage in ambient atmosphere. These devices can be easily manufactured by means of facile spray-coating techniques, which are compatible with large-area printing processes. We also demonstrated complementary inverters by combining BBL-based n-type OECTs with p-type accumulation-operating OECTs based on the conjugated polyelectrolyte poly-(3-carboxy-pentyl-thiphene) (P3CPT). This is, to the best of our knowledge, the first demonstration of complementary logic circuits with high gain based entirely on OECTs. These results show that ladder-type conducting polymers have great potential in electrochemical transistors and set material design strategies for next-generation n-type OECTs.

The electrical characteristics of BBL-based OECTs were evaluated using interdigitated gold source and drain electrodes patterned on a glass substrate. The conjugated polymer was deposited by spin coating, unless indicated otherwise, and the device was operated in an aqueous 0.1 M NaCl solution with an Ag/AgCl gate electrode. Figure 1C,D shows the output and transfer characteristics of an OECT, having a 20 nm thick BBL channel with a length L = 20 µm and a width W = 39 mm. When a positive bias voltage is applied to the gate, anions in the electrolyte insulator drift toward the electrolyte-metal gate interface, while cations penetrate the semiconductor layer, resulting in an increase in the magnitude of the current flowing in the

channel between the source and the drain electrodes. The current is modulated with the gate voltage consistent with an accumulation mode operation; that is, the current increases with increasing V_G (Figure 1C). As typical for an electrolyte-gated transistor, the device operates at low gate voltages (V_G < 0.8 V) and the current saturates when the drain voltage is increased. This allows for low-power consumption devices with high on-to-off current ratios. The transistor shows a large transconductance of 1.4 mS at $V_D = V_G = 0.6$ V (Figure 1D). At higher gate voltage, the transconductance drops as typically observed in OECTs. This nonmonotonic dependence of transconductance on gate voltage may be ascribed to the influence of disorder on the electronic transport properties of the organic semiconductor.[17]

The increase in current upon the application of a positive gate bias is consistent with the injection of Na^+ cations from the electrolyte into the BBL film, counterbalanced by the injection of electrons from the source. Further insight into the operation of the device can be obtained from the spectroelectrochemical response of the films. Spectroelectrochemistry is a well-established technique to shed light into doping mechanisms of semiconducting polymers.[18] The change of the doping level (i.e., charge density) of the material is in fact directly translated into a modification of its electronic band structure, i.e., absorption properties. **Figure 2** shows the optical absorption spectra of BBL films before and after application of a positive bias at the gate electrode. In agreement with previous report for undoped BBL, the absorption spectrum of pristine BBL films (V_G = 0 V) shows an intense peak at around 580 nm, which is associated with the S_0–S_1 transition. Upon application of a positive bias at the gate electrode, the BBL film switches from a neutral to a reduced state and two new absorption features are observed, one centered at 400 nm and then a broad band evolving at 800–900 nm. The intensity of these features increases incrementally upon applying higher positive gate voltages, while the intensity of the initial transition decreases correspondingly. The appearance of the new band at lower energy is ascribed to polaron-induced transitions. This is in agreement with the absorption spectra of molecularly n-doped BBL films,[15] and consistent with accumulation of charges in the electroactive BBL films.

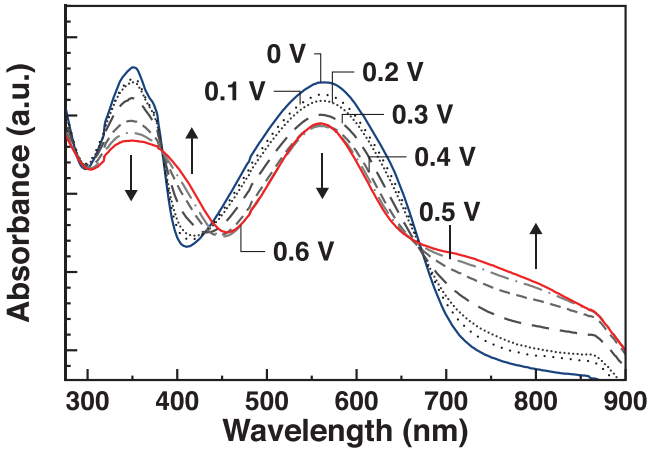

Figure 2. Spectroelectrochemistry measurements of BBL thin films recorded at different gate voltage biases ranging from 0 to 0.6 V in 0.1 M NaCl aqueous solution.

As ions penetrate into the OECT active layer, the effective capacitance of the channel strongly depends on the volume of the conducting polymer film. Therefore, the volumetric response of the capacitance leads to a dependence of the transconductance on the channel dimension.[19] For a fixed device geometry, the thickness of the active layer can then be used to tune the transconductance, and hence the performance, of the device. Thick films of BBL, ranging from 40 to 180 nm, were prepared via spray-coating depositions of an aqueous BBL dispersion (details of the preparation steps can be found in the Experimental Section). Spray-coating of conducting polymers allows for a facile printing of the active layer and it is fully compatible with large area manufacturing processes.[20] **Figure 3** reports the electrical characteristics of BBL-based OECTs having an active layer thickness d = 180 nm. The thick spray-coated BBL films are composed of interconnected networks of nanofibers with dimensions of around 100 nm in size as shown by scanning electron microscopy measurements (see Figure S2 of the Supporting Information), and in agreement with previous reports.[21] The maximum transconductance of the 180 nm thick spray-coated device is 9.7 mS, significantly higher than the spin-coated device ($g_{m,max}$ = 1.4 mS). Moreover, the device exhibits on-to-off current ratio larger than 6×10^3. When normalized for the transistor channel area (W/L = 1950), the maximum transconductance of our BBL-based OECTs is

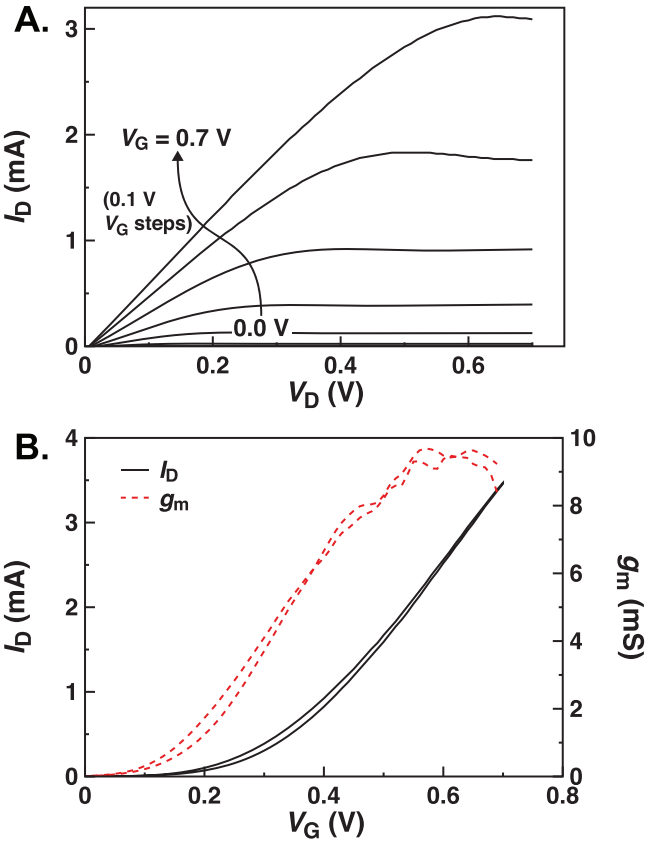

Figure 3. A) Output characteristics of an OECT (W = 39 mm, L = 20 µm, d = 180 nm) with gate voltage ranging from 0 to 0.7 V. B) Transfer characteristics of the same device and the corresponding transconductance values at V_D = 0.6 V.

about 2.5 times higher than that of recently reported NDI-based OECTs having comparable thickness (g_m = ≈4 mS, taking into account a W/L = 10). The output and transfer characteristics of the other BBL-based OECTs with different active layer thickness are shown in Figure S3 of the Supporting Information. A linear correlation is found between transconductance and active layer thickness (see Figure S4 of the Supporting Information), in agreement with previous reports.[19] The volumetric capacitance, as extracted from impedance measurements at different film thickness and V_G = 0.5 V, is ≈930 ± 40 F cm^{-3} (Figure S5, Supporting Information). Remarkably, this value exceeds more than twofold that of other NDI-based OECTs (≈400 F cm^{-3}),[10] and is several orders of magnitude higher than that estimated for n-type electrolyte-gated field-effect transistors.[22] As the transconductance is determined by the product of charge carrier mobility and capacitance per unit volume,[19] an electron mobility of about 7 × 10^{-4} cm^2 V^{-1} s^{-1} is estimated for BBL in these OECTs, which is in good agreement with the saturation mobility of 10^{-3} cm^2 V^{-1} s^{-1} measured in solid-state field-effect transistors for the same batch of polymer.[15]

One of the prime requirements when using OECTs as a recording or sensor device in biological applications is stable operation in aqueous electrolyte media, without any degradation of the active material and/or drift of the device parameters. **Figure 4**A presents the stability of the current generated in a BBL spray-coated OECT (with thickness 90 nm) at V_D = 0.5 V, upon successive gate voltage pulses (V_G = 0.5 V, pulse length = 5 s) for 1 h. No current degradation is observed during this time, thus showing that BBL has a very good operational stability in water electrolytes, as also suggested by its high EA,[15] and in good agreement with previous studies.[21,23] In addition, reversible electrochemical switching between the reduced and neutral states is observed in cyclic voltammetry measurements performed in aqueous solution, under ambient conditions and without removing oxygen, even after 500 cycles (Figure S6, Supporting Information). Atomic force microscopy shows also no visible changes in the thin film morphology (Figure S7, Supporting Information). The response time of this OECT, estimated by an exponential fit, is 0.9 and 0.2 s for the switch-on and switch-off, respectively (Figure 4B and Figure S8, Supporting Information). These values are comparable to those of other accumulation mode p-type OECTs[8b] and strongly depend on the channel layer thickness, suggesting that diffusion of ions throughout the active volume is the limiting step in our devices. This limitation could perhaps be overcome by either a miniaturization of the transistor channel[24] or by functionalizing the polymer backbone with chemical moieties that promote ion migration.[25] Although the latter approach could lead to a lowering of the active volume, hence a reduction of the volumetric capacitance, it might also influence both ions injection into the film and their effectiveness in doping the conjugated polymer, thus improving the responsiveness of our OECTs. It has been shown indeed that hydrophilic side chains favor efficient transport of ions, as compared to hydrophobic (aliphatic) side chains.[26] In addition to these advantages, side chains engineering could facilitate processing of the material. We also tested our OECTs after three months of storage in ambient atmosphere, and observed that both I_D and g_m remain unaffected (Figure S9, Supporting Information), confirming a high operational stability of BBL-based OECTs.

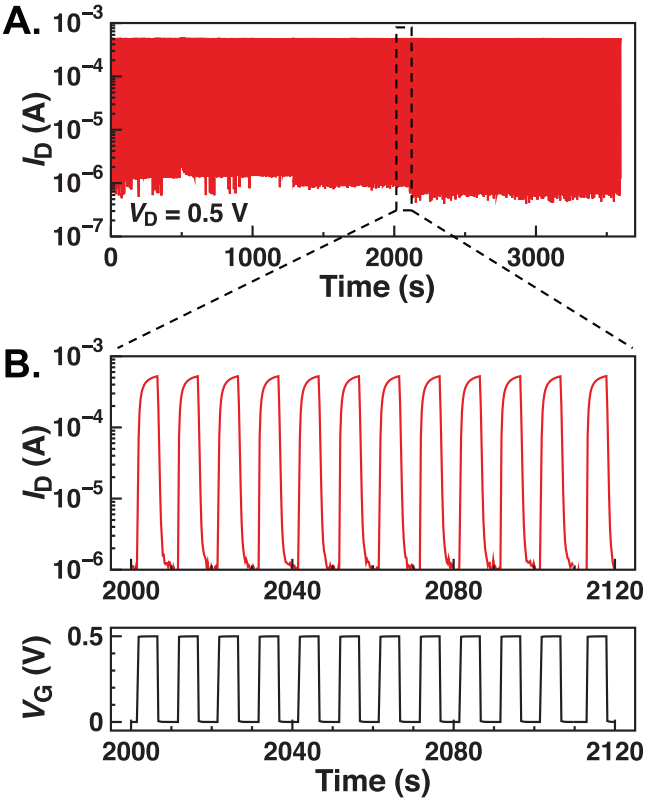

Figure 4. A) Stability test of the spray-coated OECT under sequential square wave gate voltage for 1 h (V_G = 0.5 V, pulse length = 5 s). B) 2 min enlargement at t = 2060 s; the response time, estimated by an exponential fit, is 0.9 and 0.2 s for the switch-on and switch-off, respectively (see Figure S8 in the Supporting Information).

The complementary inverter represents a simple logic circuit that can be built by combining an n-type and a p-type OECT.[27] The circuit layout of a complementary inverter is shown in the inset of **Figure 5**C, where the *n*-channel (*n*, pull-down transistor), across which the output voltage is measured, is connected to a *p*-channel (*p*, pull-up transistor). In this circuit configuration, a change in the voltage bias, applied to a common gate, is expressed as a change in the voltage drop across the circuit. First, we fabricated p-type OECTs based on the hole-transporting material P3CPT. The chemical structure of P3CPT is reported in the inset of Figure 5B. P3CPT is a well-known p-type semiconducting polymer, which has been reported to work as an efficient and highly stable electroactive channel material in accumulation-mode OECTs.[25] Figure 5A,B shows the output and transfer characteristics of an OECT having a 30 nm thick P3CPT with a channel width W = 39 mm and length L = 20 µm, respectively. When a negative bias voltage is applied to the gate, anions from the electrolyte diffuse within the semiconductor layer, while cations drift toward the electrolyte-metal gate interface. This results in an electrochemical doping of P3CPT and a consequent increase of the drain current by several orders of magnitude. Thus, the transistor works in the accumulation mode (Figure 5A). The transconductance reaches values as high as 13.3 mS at V_D = V_G = 0.6 V (Figure 5B).

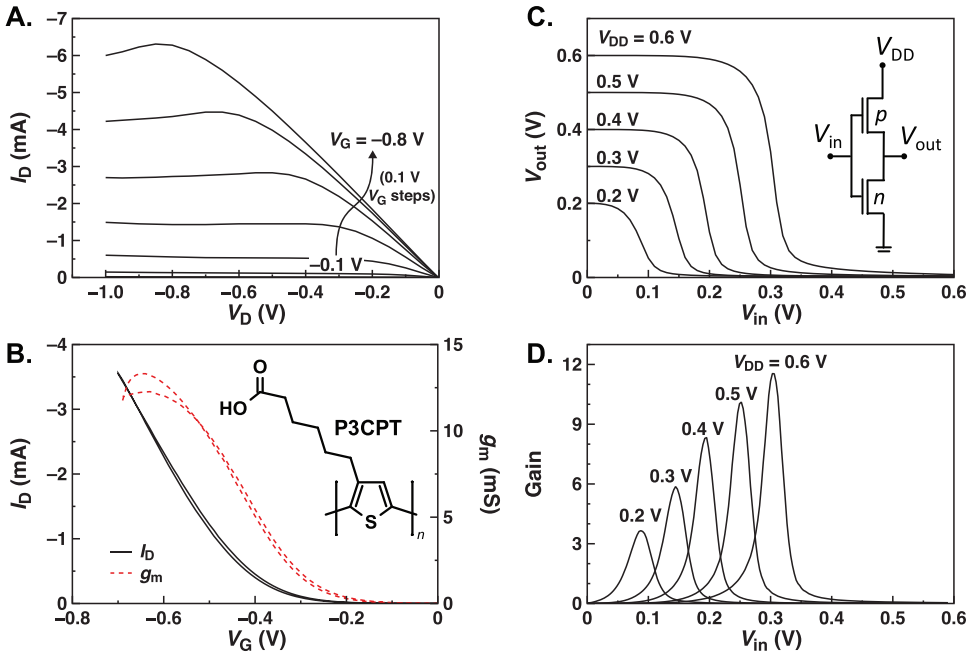

Figure 5. A) Output and B) transfer characteristics of the p-type P3CPT-based ECT. The transfer curve reported in (B) was tested under V_D = –0.6 V. C) Input–output characteristics of a typical complementary-like inverter and D) corresponding voltage gains ($\partial V_{out}/\partial V_{in}$) of the inverters. The inset in (C) shows a schematic representation of the inverter.

The p-type P3CPT-based OECT was then connected by external wiring to the n-type BBL-based transistor to form the complementary inverter. The thickness of the BBL-based OECT was such that the device transconductance could match that of the p-type OECT. The resulting inverter characteristics are given in Figure 5C. When the supply voltage (V_{DD}) is set to 0.6 V and the input voltage (V_{in}) is swept from 0 to 0.6 V, a relatively high gain value, larger than 11, is obtained (Figure 5D). Here, gain is defined as $\partial V_{out}/\partial V_{in}$. Note that the switching voltage of the inverter ($V_{out} = V_{in}$) is about the ideal $V_{DD}/2$, since the ambipolar charge transport is almost perfectly balanced. This results in a large worst-case noise margin (NM) of 0.2 V at V_{DD} = 0.6 V. The latter is ≈67% of its maximum theoretical value (at V_{DD} = 0.6 V) given as $NM_{max} = V_{DD}/2$ = 0.3 V. These values are substantially larger than those reported for p-MOS inverters used in complex circuitry[28] and among the best based on solution-processed organic CMOS-like inverters operating at such a low supply voltage (V_{DD} = 0.6 V).[22] The inverter is the most basic element in circuits and it is used to construct logic gates and amplifiers. As a biological event (e.g., an electrophysiological signal[4a] or an enzymatic reaction[3a]) modifies the effective gate bias, the inherent gain of our complementary-like inverters can then be used as an amplifying transducer to enhance the recorded signal with low power consumption.

In conclusion, we demonstrated that ladder-type conducting polymers such as BBL can function as efficient electroactive materials for OECTs. The transistors can be fabricated by means of facile spray-coating techniques and work in accumulation mode with record high transconductance for n-type OECTs. Because of the high electron conductivity and EA, BBL-based OECTs can operate with high current in water and show a high stability during pulse measurements over 1 h, as well as remarkable ambient stability over three months of storage in air. We also demonstrated complementary inverters by combining the best-performing BBL-based n-type OECTs with p-type OECTs based on conjugated polyelectrolytes such as P3CPT. This is, to the best of our knowledge, the first demonstration of complementary logic circuits with high gains based entirely on electrochemical operation. These results show that ladder-type conducting polymers are a class of electroactive materials with great potential for applications in electrochemical transistors.

Experimental Section

Film Preparation: All devices were fabricated on glass substrates cleaned sequentially in acetone, water, and isopropanol, followed by the drying step with nitrogen. The glass substrates were purchased from Micrux Technologies, with prepatterned interdigitated gold electrodes given a channel length of 20 µm and a channel width of 39 mm. The electrolyte was a 0.1 M NaCl water solution while the gate electrode was an Ag/AgCl wire immersed in the electrolyte. BBL and methanesulfonic acid (MSA) (>99%) were purchased from Sigma-Aldrich. For spin-coated films, BBL was dissolved in MSA at the concentration of 5 mg mL^{-1}. The solution was stirred at 70 °C for ≈1 h to allow complete dissolution of the polymer. After stirring, the solution was spin-coated onto the glass substrates at 1000 rpm for 1 min. The BBL films were then soaked immediately after spin-coating into deionized water to remove MSA for 1 h, and then dried on a hot plate at 200 °C for 1 h. The resulting film thickness was about 20 nm. P3CPT was purchased from Rieke Metals Inc. and dissolved in dimethyl sulfoxide at a concentration of 15 mg mL^{-1}, stirring overnight on the hot plate at 70 °C to fully dissolve the polymer. Then the solution was dropped on prepatterned glass substrate and spin-coated at a speed of 2000 rpm for 2 min, yielding a film thickness of about 30 nm. Spray-coated films were prepared following a procedure

reported in the literature (see the Supporting Information for a detailed procedure). In brief, a very diluted BBL in MSA was injected through a 100 µm diameter pipette into a 0.5 wt% solution of IGEPAL co-520 in water while stirring. BBL precipitates in contact with water. The precipitate was broken by ultrasonic for 1.5 h. The BBL particles were then washed several times with water via a centrifugation/dispersion cycle until the supernatant was no longer acidic. The precipitate was finally dispersed in water, sonicated again for 1.5 h, and filtered with a 10 µm pore-diameter syringe filter. The resulting BBL suspension was kept at a concentration at about 2 mg mL^{-1}. The BBL suspension was spay-coated by means of a commercially available air brush on top of the clean glass substrates kept at 200 °C on a hotplate. One layer of BBL was prepared by spraying 0.5 mL of the prepared BBL dispersion for 30 s. This step was repeated several times to get thicker films. After spray-coating, the films were immersed in a nitric acid bath (0.5 M) and left under stirring for 1 h to remove the residential IGEPAL. Later, the films were dried on the hot plate at 200 °C. The film thickness was measured by Dektak surface profilometer.

Optical and Electrical Characterization: Absorption spectra of BBL were conducted at room temperature using a UV–vis spectrophotometer (PerkinElmer Lambda 900). The electrical characterization of the OECTs and inverters was carried out by means of a Keithley 4200 semiconductor parameter analyzer. For the stability test, the sequential gate pulse was applied via a Tektronix 3390 wave-function generator.

Supporting Information

Supporting Information is available from the Wiley Online Library or from the author.

Acknowledgements

The authors acknowledge support from the Knut and Alice Wallenberg Foundation (project "Tail of the sun") and the Swedish Foundation for Strategic Research (Synergy project). S.F. gratefully acknowledges funding by the Swedish Governmental Agency for Innovation Systems – VINNOVA (Grant No. 2015-04859), the Swedish Research Council (Grant No. 2016-03979), and the Advanced Functional Materials Center at Linköping University (Grant No. 2009-00971).

Conflict of Interest

The authors declare no conflict of interest.

Keywords

accumulation mode OECTs, ladder-type polymers, n-type polymers, transconductance

Received: August 27, 2017
Revised: November 23, 2017
Published online: January 10, 2018

[1] a) D. Nilsson, N. Robinson, M. Berggren, R. Forchheimer, *Adv. Mater.* **2005**, *17*, 353; b) P. Andersson, R. Forchheimer, P. Tehrani, M. Berggren, *Adv. Funct. Mater.* **2007**, *17*, 3074; c) M. Hamedi, R. Forchheimer, O. Inganas, *Nat. Mater.* **2007**, *6*, 357; d) E. Mitraka, L. Kergoat, Z. U. Khan, S. Fabiano, O. Douheret, P. Leclere, M. Nilsson, P. Andersson Ersman, G. Gustafsson, R. Lazzaroni, M. Berggren, X. Crispin, *J. Mater. Chem. C* **2015**, *3*, 7604; e) S. Fabiano, N. Sani, J. Kawahara, L. Kergoat, J. Nissa, I. Engquist, X. Crispin, M. Berggren, *Sci. Adv.* **2017**, *3*, e1700345; f) C. Qian, J. Sun, L.-a. Kong, G. Gou, J. Yang, J. He, Y. Gao, Q. Wan, *ACS Appl. Mater. Interfaces* **2016**, *8*, 26169; g) Y. van de Burgt, E. Lubberman, E. J. Fuller, S. T. Keene, G. C. Faria, S. Agarwal, M. J. Marinella, A. Alec Talin, A. Salleo, *Nat. Mater.* **2017**, *16*, 414; h) P. Gkoupidenis, D. A. Koutsouras, G. G. Malliaras, *Nat. Commun.* **2017**, *8*, 15448.

[2] a) M. Berggren, A. Richter-Dahlfors, *Adv. Mater.* **2007**, *19*, 3201; b) L. Kergoat, B. Piro, D. T. Simon, M.-C. Pham, V. Noël, M. Berggren, *Adv. Mater.* **2014**, *26*, 5658; c) D. Zhao, S. Fabiano, M. Berggren, X. Crispin, *Nat. Commun.* **2017**, *8*, 14214; d) M. Braendlein, A.-M. Pappa, M. Ferro, A. Lopresti, C. Acquaviva, E. Mamessier, G. G. Malliaras, R. M. Owens, *Adv. Mater.* **2017**, *29*, 1605744.

[3] a) E. Bihar, Y. Deng, T. Miyake, M. Saadaoui, G. G. Malliaras, M. Rolandi, *Sci. Rep.* **2016**, *6*, 27582; b) K. Manoli, M. Magliulo, M. Y. Mulla, M. Singh, L. Sabbatini, G. Palazzo, L. Torsi, *Angew. Chem., Int. Ed.* **2015**, *54*, 12562; c) G. Palazzo, D. De Tullio, M. Magliulo, A. Mallardi, F. Intranuovo, M. Y. Mulla, P. Favia, I. Vikholm-Lundin, L. Torsi, *Adv. Mater.* **2015**, *27*, 911.

[4] a) A. Campana, T. Cramer, D. T. Simon, M. Berggren, F. Biscarini, *Adv. Mater.* **2014**, *26*, 3874; b) C. Yao, Q. Li, J. Guo, F. Yan, I. M. Hsing, *Adv. Healthcare Mater.* **2015**, *4*, 528.

[5] a) L. H. Jimison, S. A. Tria, D. Khodagholy, M. Gurfinkel, E. Lanzarini, A. Hama, G. G. Malliaras, R. M. Owens, *Adv. Mater.* **2012**, *24*, 5919; b) S. Desbief, M. di Lauro, S. Casalini, D. Guerin, S. Tortorella, M. Barbalinardo, A. Kyndiah, M. Murgia, T. Cramer, F. Biscarini, D. Vuillaume, *Org. Electron.* **2016**, *38*, 21.

[6] a) R. Giridharagopal, L. Q. Flagg, J. S. Harrison, M. E. Ziffer, J. Onorato, C. K. Luscombe, D. S. Ginger, *Nat. Mater.* **2017**, *16*, 737; b) J. O. Guardado, A. Salleo, *Adv. Funct. Mater.* **2017**, *27*, 1701791.

[7] a) D. Khodagholy, J. Rivnay, M. Sessolo, M. Gurfinkel, P. Leleux, L. H. Jimison, E. Stavrinidou, T. Herve, S. Sanaur, R. M. Owens, G. G. Malliaras, *Nat. Commun.* **2013**, *4*, 2133; b) J. Edberg, H. Granberg, Z. U. Khan, J. W. Andreasen, X. Liu, D. Zhao, H. Zhang, Y. Yao, J. W. Brill, I. Engquist, M. Fahlman, L. Wågberg, X. Crispin, M. Berggren, *Adv. Sci.* **2016**, *3*, 1500305.

[8] a) S. Inal, J. Rivnay, P. Leleux, M. Ferro, M. Ramuz, J. C. Brendel, M. M. Schmidt, M. Thelakkat, G. G. Malliaras, *Adv. Mater.* **2014**, *26*, 7450; b) E. Zeglio, M. Vagin, C. Musumeci, F. N. Ajjan, R. Gabrielsson, X. T. Trinh, N. T. Son, A. Maziz, N. Solin, O. Inganäs, *Chem. Mater.* **2015**, *27*, 6385.

[9] H. Usta, A. Facchetti, T. J. Marks, *Acc. Chem. Res.* **2011**, *44*, 501.

[10] A. Giovannitti, C. B. Nielsen, D.-T. Sbircea, S. Inal, M. Donahue, M. R. Niazi, D. A. Hanifi, A. Amassian, G. G. Malliaras, J. Rivnay, I. McCulloch, *Nat. Commun.* **2016**, *7*, 13066.

[11] R. Di Pietro, D. Fazzi, T. B. Kehoe, H. Sirringhaus, *J. Am. Chem. Soc.* **2012**, *134*, 14877.

[12] G.-S. Ryu, Z. Chen, H. Usta, Y.-Y. Noh, A. Facchetti, *MRS Commun.* **2016**, *6*, 47.

[13] a) D. Fazzi, M. Caironi, C. Castiglioni, *J. Am. Chem. Soc.* **2011**, *133*, 19056; b) G. Wetzelaer, M. Kuik, Y. Olivier, V. Lemaur, J. Cornil, S. Fabiano, M. A. Loi, P. W. M. Blom, *Phys. Rev. B* **2012**, *86*, 165203; c) B. D. Naab, X. Gu, T. Kurosawa, J. W. F. To, A. Salleo, Z. Bao, *Adv. Electron. Mater.* **2016**, *2*, 1600004.

[14] A. Babel, S. A. Jenekhe, *J. Am. Chem. Soc.* **2003**, *125*, 13656.

[15] S. Wang, H. Sun, U. Ail, M. Vagin, P. O. Å. Persson, J. W. Andreasen, W. Thiel, M. Berggren, X. Crispin, D. Fazzi, S. Fabiano, *Adv. Mater.* **2016**, *28*, 10764.

[16] Y. Liang, Z. Chen, Y. Jing, Y. Rong, A. Facchetti, Y. Yao, *J. Am. Chem. Soc.* **2015**, *137*, 4956.
[17] J. T. Friedlein, J. Rivnay, D. H. Dunlap, I. McCulloch, S. E. Shaheen, R. R. McLeod, G. G. Malliaras, *Appl. Phys. Lett.* **2017**, *111*, 023301.
[18] a) C. A. Thomas, K. Zong, K. A. Abboud, P. J. Steel, J. R. Reynolds, *J. Am. Chem. Soc.* **2004**, *126*, 16440; b) J. A. Kerszulis, C. M. Amb, A. L. Dyer, J. R. Reynolds, *Macromolecules* **2014**, *47*, 5462.
[19] J. Rivnay, P. Leleux, M. Ferro, M. Sessolo, A. Williamson, D. A. Koutsouras, D. Khodagholy, M. Ramuz, X. Strakosas, R. M. Owens, C. Benar, J.-M. Badier, C. Bernard, G. G. Malliaras, *Sci. Adv.* **2015**, *1*, e1400251.
[20] Y. Xia, W. Zhang, M. Ha, J. H. Cho, M. J. Renn, C. H. Kim, C. D. Frisbie, *Adv. Funct. Mater.* **2010**, *20*, 587.
[21] P. Bornoz, M. S. Prévot, X. Yu, N. Guijarro, K. Sivula, *J. Am. Chem. Soc.* **2015**, *137*, 15338.
[22] a) L. Herlogsson, X. Crispin, S. Tierney, M. Berggren, *Adv. Mater.* **2011**, *23*, 4684; b) R. Porrazzo, A. Luzio, S. Bellani, G. E. Bonacchini, Y.-Y. Noh, Y.-H. Kim, G. Lanzani, M. R. Antognazza, M. Caironi, *ACS Omega* **2017**, *2*, 1.
[23] H. Antoniadis, M. A. Abkowitz, J. A. Osaheni, S. A. Jenekhe, M. Stolka, *Chem. Mater.* **1994**, *6*, 63.
[24] L. Herlogsson, Y. Y. Noh, N. Zhao, X. Crispin, H. Sirringhaus, M. Berggren, *Adv. Mater.* **2008**, *20*, 4708.
[25] A. Laiho, L. Herlogsson, R. Forchheimer, X. Crispin, M. Berggren, *Proc. Natl. Acad. Sci. USA* **2011**, *108*, 15069.
[26] A. Giovannitti, D.-T. Sbircea, S. Inal, C. B. Nielsen, E. Bandiello, D. A. Hanifi, M. Sessolo, G. G. Malliaras, I. McCulloch, J. Rivnay, *Proc. Natl. Acad. Sci. USA* **2016**, *113*, 12017.
[27] K. J. Baeg, M. Caironi, Y. Y. Noh, *Adv. Mater.* **2013**, *25*, 4210.
[28] J. H. Cho, J. Lee, Y. Xia, B. Kim, Y. Y. He, M. J. Renn, T. P. Lodge, C. D. Frisbie, *Nat. Mater.* **2008**, *7*, 900.